

EUROPEAN ORGANIZATION FOR NUCLEAR RESEARCH

Proposal to the ISOLDE and Neutron Time-of-Flight Committee

(Following HIE-ISOLDE Letter of Intent I-111)

**2<sup>+</sup> Anomaly and Configurational Isospin Polarization of <sup>136</sup>Te**

October 7, 2014

C. Stahl<sup>1</sup>, V. Werner<sup>1</sup>, N. Pietralla<sup>1</sup>, G. Rainovski<sup>2</sup>, A. Jungclaus<sup>3</sup>, T. Kröll<sup>1</sup>,  
M. Lettmann<sup>1</sup>, O. Möller<sup>1</sup>, M. Reese<sup>1</sup>, R. Stegmann<sup>1</sup>, T. Stora<sup>4</sup>

<sup>1</sup>*Institut für Kernphysik, Technische Universität Darmstadt, 64289 Darmstadt, Germany*

<sup>2</sup>*Faculty of Physics, St. Kliment Ohridski University of Sofia, 1164 Sofia, Bulgaria*

<sup>3</sup>*Instituto de Estructura de la Materia, CSIC, 28006 Madrid, Spain*

<sup>4</sup>*CERN, Switzerland*

**Spokesperson:** V. Werner (vw@ikp.tu-darmstadt.de)

**Co-Spokespersons:** N. Pietralla (pietralla@ikp.tu-darmstadt.de)

G. Rainovski (rig@phys.uni-sofia.bg)

**Contact person:** E. Rapisarda (elisa.rapisarda@cern.ch)

**Abstract:**

It is proposed to perform a Coulomb excitation experiment on beams of radioactive ions of <sup>136</sup>Te delivered by HIE-ISOLDE impinging on a <sup>58</sup>Ni target. Scattered particles will be detected by a DSSTD detector and  $\gamma$  rays will be detected by the MINIBALL array. The proposed Configurational Isospin Polarization (CIP) of the two lowest 2<sup>+</sup> states will be determined by measuring the *E2* excitation yield distribution to them. The expected proton-dominated one-phonon character of the second excited 2<sup>+</sup> state of <sup>136</sup>Te will be tested on the basis of absolute electromagnetic matrix elements from the observed Coulomb excitation cross sections. Complementary lifetime information on this predominant 2<sub>1,ms</sub><sup>+</sup> state will be extracted using the differential DSAM technique. The experiment will clarify to what extent CIP is responsible for the 2<sup>+</sup> anomaly in <sup>136</sup>Te.

**Requested shifts:** 9 shifts

**Installation:** MINIBALL + CD-only



# 1 Introduction

Of particular interest of contemporary nuclear structure research is the impact of local shell structure on the proton-neutron (pn) balance of low-energy  $2^+$  states at the onset of collectivity near neutron rich shell closures, such as  $^{78}\text{Ni}$  or  $^{132}\text{Sn}$ . Two fundamental one-phonon quadrupole excitations are usually found in near-spherical nuclei, both mixtures of the underlying seniority-2 proton and neutron  $2^+$  configurations, which can be simplified into a two-state mixing scenario:  $|2_i^+\rangle = \alpha_i |2_\pi^+\rangle \pm \beta_i |2_\nu^+\rangle$ . Near stability, one is a fully-symmetric state (FSS), the  $2_1^+$  state, resulting from an in-phase combination of proton and neutron contributions. The other one is the pn-mixed-symmetry  $2_{1,\text{ms}}^+$  state [1], with the opposite phase – the lowest-energy isovector quadrupole excitation in the valence shell. Mixed-symmetry states (MSSs) are uniquely identified experimentally [2] by their strong isovector  $M1$  decay to the low-lying, fully-symmetric states (FSS). MSSs are sensitive to both the residual p-n interaction  $V_{\pi\nu}$  [3, 4] and the underlying shell structure [2, 5]. The absolute  $B(M1; 2_{1,\text{ms}}^+ \rightarrow 2_1^+)$  strength probes the relative p-n contributions in the wave functions. A mechanism dubbed Configurational Isospin Polarization (CIP) [6] occurs when proton and neutron amplitudes in the one-phonon  $2^+$  state wave functions are not balanced, and either one dominates. This phenomenon may occur near shell closures with neutron excess, such as  $^{90}\text{Zr}$  [6, 7] or  $^{132}\text{Sn}$ .

Significant CIP was found to manifest in a reduction of absolute  $M1$  rates between the two one-phonon  $2^+$  states and a simultaneous increase of  $E2$  excitation strength of that  $2^+$  state with dominant proton contribution.  $B(E2)$  strengths for both states and the  $M1$  strength between them are needed in order to uniquely quantify the amount of CIP. Recently, CIP was held responsible [8, 9] for the occurrence of the  $2^+$  anomaly observed in  $^{136}\text{Te}$  [10]. Overall, the two lowest one-phonon, predominantly FS and MS,  $2^+$  states provide a tool to *quantitatively study the p-n balance* of collective nuclear states. The latter is essential in understanding the nuclear many-body system at neutron excess.

# 2 Physics Case

With increase of the neutron excess, dramatic changes in nuclear properties can be expected. A good example is found in  $^{136}\text{Te}$ , where a simultaneous reduction of the  $E_x(2_1^+)$  excitation energy and the  $B(E2; 2_1^+ \rightarrow 0_1^+)$  transition probability with respect to the lighter isotopes is observed [10], which clearly violates the empirical rules for properties of quadrupole collective states [11, 12]. Next to  $^{132}\text{Sn}$  this phenomenon is considered "the  $2^+$  anomaly of  $^{136}\text{Te}$ ". The significant lowering of the  $B(E2; 2_1^+ \rightarrow 0_1^+)$  value in  $^{136}\text{Te}$  with respect to  $^{132}\text{Te}$  implies considerably different structures for the  $2_1^+$  states of these nuclei. It has been suggested [13, 14, 15] that neutron dominance, i.e., CIP, occurs in the wave function of the  $2_1^+$  state of  $^{136}\text{Te}$ , leading to this anomalous behavior. Similarly to findings in  $^{92,94}\text{Zr}$  [7], this pn asymmetry in  $^{136}\text{Te}$  can be a combined effect of the asymmetry in the excitation energies of the basic  $2^+$  proton [ $E_x(2_1^+; ^{134}\text{Te}) = 1279$  keV] and neutron [ $E_x(2_1^+; ^{134}\text{Sn}) = 762$  keV] configurations and a weak pn interaction which cannot compensate for that energy difference by sufficiently strong mixing [14]. In contrast, the excitation energy of the basic neutron  $2^+$  configuration in  $^{132}\text{Te}$  [ $E_x(2_1^+; ^{130}\text{Sn}) = 1221$  keV] is compa-

rable to that of the basic proton  $2^+$  configuration [ $E_x(2_1^+; ^{134}\text{Te}) = 1279$  keV], suggesting a more balanced pn composition for the  $^{132}\text{Te}$   $2_1^+$  state. However, the availability of two proton orbitals  $1g_{7/2}$  and  $2d_{5/2}$  as compared to the Zr isotopes, where only  $2g_{9/2}$  is open and CIP has been experimentally established, may lead to a significant  $B(M1; 2_2^+ \rightarrow 2_1^+)$  transition strength in  $^{136}\text{Te}$ , and a large  $B(E2; 0_1^+ \rightarrow 2_2^+)$  excitation strength from the ground state. Measurements of these observables are urgently needed for both states –  $2_1^+$  and  $2_2^+$  – in order to better understand their structure. The expected manifestation of the CIP mechanism in the Te isotopes can be summarized as follows:

- The wave functions of the one-phonon  $2^+$  FSS and MSS of  $^{132}\text{Te}$  have balanced p-n character. As a result, the  $B(E2; 2_1^+ \rightarrow 0_1^+)$  value follows the expected trend, and the  $2_{1,\text{ms}}^+$  state decays with a strong  $M1$  transition to the  $2_1^+$  state. These two expectations are already proven experimentally [10, 8].
- In  $^{136}\text{Te}$ , the wave functions of the  $2_1^+$  and  $2_{1,\text{ms}}^+$  states are neutron and proton dominated, respectively. As a result, the  $B(E2; 2_1^+ \rightarrow 0_1^+)$  value of  $^{136}\text{Te}$  is suppressed with respect to that of  $^{132}\text{Te}$ , and the  $2_{1,\text{ms}}^+$  state is expected to decay with a weaker  $M1$  transition to the  $2_1^+$  state, and with an enhanced  $E2$  transition to the ground state. The newest theoretical calculations in the framework of the quasi-particle random phase approximation published just recently [9] predict values of  $B(M1; 2_2^+ \rightarrow 2_1^+) = 0.51 \mu_N^2$  and  $B(E2; 0_1^+ \rightarrow 2_2^+) = 740 \text{ e}^2\text{b}^2$ .

The new experimental data on FS and MSSs in the mass  $A \approx 130$  region [2, 4, 5, 8] have inspired extended theoretical studies in the framework of the most advanced microscopic nuclear models [8, 16, 17, 18, 19, 20]. Very recently, it has been predicted that the pn exchange symmetry is strongly broken as Te and Xe isotopes depart from doubly-magic  $^{132}\text{Sn}$  [20]. However, in Ref. [20], the authors clearly state that it is crucial to test the shell model predictions experimentally. In essence, this calls for experiments to measure  $B(E2)$  and  $B(M1)$  strengths of the two lowest  $2^+$  states. This task received further importance from the recent observation [8] that the previous  $B(E2)$  result on the  $2_1^+$  state alone of  $^{136}\text{Te}$  from Oak Ridge is inaccurate due to an erroneous assumption of target thickness. Currently, such an experiment on the first two  $2^+$  states of  $^{136}\text{Te}$  can neither be done at Oak Ridge (due to shut-down) nor at the CARIBU facility at Argonne National Laboratory (due to too high beam contamination with stable  $^{136}\text{Xe}$  until a new EBIS will be installed in 2016/17) nor at RIKEN or GSI (due to insufficient  $\gamma$ -ray energy resolution for the off-yrast states). However, the  $2^+$  anomaly in  $^{136}\text{Te}$  and its configurational isospin polarization can quantitatively be solved for good at the MINIBALL at HIE-Isolde facility at CERN at this point already. This measurement will have a significant impact on our understanding of the onset of quadrupole-collectivity near neutron-rich shell closures. Therefore, we propose an experiment using projectile-Coulomb excitation of the nucleus  $^{136}\text{Te}$  produced by ISOLDE using the MINIBALL detector array in conjunction with the standard DSSSD "CD"-detector.

### 3 Feasibility of the proposed experiment

We propose a combined experiment using the well-established technique of sub-barrier projectile Coulomb excitation to extract the electromagnetic matrix elements of transitions between excited states in  $^{136}\text{Te}$  and, simultaneously, a variant of the Doppler Shift Attenuation Method [21, 22] (DSAM) for extraction of the lifetimes of short-lived states of  $^{136}\text{Te}$  projectile nuclei.

The  $^{136}\text{Te}$  ions will be produced by ISOLDE with a standard  $\text{UC}_x/\text{graphite}$  target.  $^{136}\text{Te}$  ions can be extracted with intensities  $> 4 \cdot 10^7$  ions/ $\mu\text{C}$  from the  $\text{UC}_x/\text{graphite}$  target target [24]. They will be charge-bred by REX-EBIS and accelerated by the HIE-LINAC to energies of 510 MeV (3.75 MeV/u). A considerable contamination of the beam with isobaric ions, in particular  $^{136}\text{Xe}$ , may persist after charge-breeding. Therefore, we intend to use selective schemes for which a special development has been approved already in the past (proposal by T. Kröll et al. on  $^{142}\text{Xe}$  and development of Te beams). Two options need to be investigated: either the classical way in which a molecular compound will be formed in the plasma ion source and broken-up later on acceleration in the LINAC, or selective laser ionization in the presence of a functional element. According to the RILIS database [23], ionization schemes for Tellurium were tested with the Ti:Sa lasers. Beam intensities of  $> 10^5$  ions/s can conservatively be assumed to be available on the secondary  $^{58}\text{Ni}$  target with a thickness of 3 mg/cm<sup>2</sup> at the focus of MINIBALL. Both projectile and target nuclei will be excited via Coulomb excitation in the scattering process. The scattered nuclei will be detected by the annular CD detector placed 20 mm behind the secondary target and covering scattering angles of 24-64 degrees in the laboratory system and of 51-131 degrees in the center-of-mass system of the scattered target nuclei. The reaction kinematics is shown in Fig. 1. Only recoiling target-nuclei will be detected in the DSSSD. The energy of the projectile ions has been chosen such that safe Coulomb excitation is ensured for all scattering angles covered by the DSSSD. Deexcitation  $\gamma$ -rays will be detected by the MINIBALL array. Background will be suppressed by demanding particle-gamma coincidences.

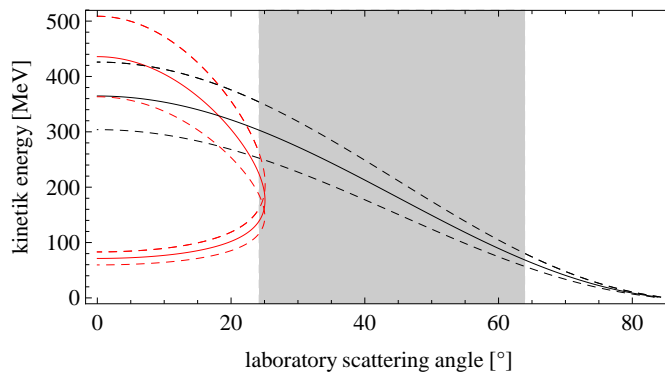


Figure 1: *Inverse kinematics plot for  $^{136}\text{Te}$  at 3.75 MeV/u impinging on a 3 mg/cm<sup>2</sup>  $^{58}\text{Ni}$  target. The kinematics is shown for the beam energy at entrance and exit of the target (dashed lines) and at the center of the target (solid lines). The angular range covered by the DSSSD is indicated by the shaded area. Only scattered target-nuclei will be detected.*

The electromagnetic matrix elements for the transitions in the projectile nucleus  $^{136}\text{Te}$  will be extracted from a fit of the matrix elements to the experimentally observed  $\gamma$ -ray yields. A normalization can be performed either on the re-analyzed  $B(E2; 2_1^+ \rightarrow 0_1^+) = 5.9(9)$  W.u. of  $^{136}\text{Te}$  [8] or on the well-known value of  $B(E2; 2_1^+ \rightarrow 0_1^+)$  of  $^{58}\text{Ni}$ , thereby checking the reanalyzed Oak Ridge-data.

Complementary lifetime information on the short-lived states of  $^{136}\text{Te}$  will be extracted using the differential DSAM technique [21, 22]. This type of analysis is already well-established for stopped ion beams and can be adopted for in-flight  $\gamma$ -ray emission, i.e. without stopping the beam in the target. The method is based on the velocity-dependent Doppler shift of  $\gamma$ -rays emitted by ions in flight.

Nuclei that are excited to very short-lived states have a considerable probability of decaying before their passage through the target material is completed – in contrast to long-lived states, which are most likely to decay when the projectile ions are already behind the target. In the latter case, the velocity distribution of the emitting nuclei for a given scattering angle is very sharp – close to a delta function, leading to a sharp peak after applying the Doppler correction for the ion velocities behind the target. On the contrary, the  $\gamma$ -rays from fast decays are emitted at varying velocities with a well-defined distribution depending on the stopping power of the target material, the target thickness and the level-lifetime. Because the individual ion velocities at the time of de-excitation are not directly accessible, the known ion velocities behind the target have to be assumed in the Doppler-correction. This results in a characteristic line shape in the Doppler-corrected  $\gamma$ -ray spectrum, comparable to the line shape of the well-known DSAM measurements using stopped beams, although less strongly pronounced. In the analysis of the data, the computer code APCAD [22] will be used to calculate the velocity distribution of the ions and to perform a fit of the lifetime to the observed angular-dependent line shapes in the  $\gamma$ -ray spectra. To ensure a significant lifetime-effect on the line shape, the passage-time of the projectiles through the target has to be on the same order of magnitude as the

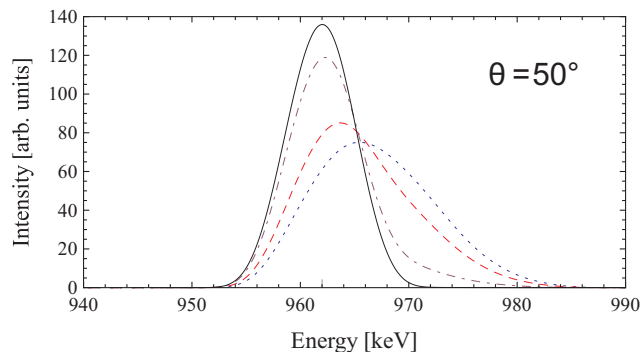


Figure 2: *Simulated line shapes of the decay line of the 962-keV  $2_{1,ms}^+ \rightarrow 2_1^+$  transition for a single MINIBALL crystal placed at  $\theta = 50^\circ$ . The line shapes for a level lifetime of 50 fs (blue dotted line) and for the expected lifetime of 100 fs (red dashed line) show a considerable effect while the line shapes for lifetimes of 500 fs (purple dash-dotted line) and 40 ps (black solid line; corresponds to  $\tau(2_1^+)$ ) are barely affected.*

lifetime of the emitting state. The  $2_{1,\text{ms}}^+$  state is an ideal candidate to be investigated using this method. Due to the large  $M1$  transition to the  $2_1^+$  state, it is expected to decay after a lifetime of  $\approx 100$  fs. This number is also predicted by the recent calculations of [9]. A target thickness of  $3 \text{ mg/cm}^2$  of Ni is therefore needed to be sensitive. The average angular straggling of the beam caused by the  $3 \text{ mg/cm}^2$  Nickel target is only around twice as large as for a  $1 \text{ mg/cm}^2$  Nickel target (according to calculations with ATIMA [25]). An illustration of the simulated line shape of the decay of the  $2_{1,\text{ms}}^+ \rightarrow 2_1^+$  transition for an assumed lifetime of 100 fs is shown in Fig. 2. **We want to stress that the lifetime measurement does not hinder the Coulex analysis.** In addition, we intend to analyze the  $\gamma$ -ray angular distribution of the decay of the  $2_1^+$  (and if possible  $2_{1,\text{ms}}^+$ ) states in order to perform a RIV analysis to extract absolute magnetic moments that will sensitively test the neutron character of the  $2_1^+$  state.

Estimates for the expected count rates have been performed using the standard Coulex code CLX. The energy loss in the target and its influence on the excitation cross-sections were taken into account. The estimates are based on the results of the recent theoretical predictions [9] of  $B(E2; 0_1^+ \rightarrow 2_{1,\text{ms}}^+) = 740 \text{ e}^2\text{fm}^4$  and  $B(E2; 2_{1,\text{ms}}^+ \rightarrow 2_1^+) = 20 \text{ e}^2\text{fm}^4$ . According to the calculations of [9], the  $2_{1,\text{ms}}^+$  state has been assumed to be the second excited  $2^+$  state of  $^{136}\text{Te}$ , which resides at an energy of 1568 keV. The  $\gamma$ -ray detection efficiency of MINIBALL has been assumed to amount to a total of 5%. Based on these considerations, we expect 558 counts per day for the decay of the  $2_{1,\text{ms}}^+$  state and 4700 counts per day for the decay of the  $2_1^+$  state of  $^{136}\text{Te}$ . Details are given in Table 1.

Table 1: Overview of the estimate for the expected count rates for projectile Coulomb excitation of  $^{136}\text{Te}$  on a  $3 \text{ mg/cm}^2$  nickel target.

| state               | $E_x$<br>(keV) | $B(\sigma\lambda)$                    |                 |                                   | cross section <sup>1</sup><br>(mb) | est. yield <sup>2</sup><br>(cts/day) |
|---------------------|----------------|---------------------------------------|-----------------|-----------------------------------|------------------------------------|--------------------------------------|
|                     |                | transition                            | $\sigma\lambda$ | value                             |                                    |                                      |
| $2_1^+$             | 606 keV        | $0_1^+ \rightarrow 2_1^+$             | E2              | $1220 \text{ e}^2\text{fm}^4$ [8] | 353 mb                             | 4700                                 |
| $2_{1,\text{ms}}^+$ | 1568 keV       | $0_1^+ \rightarrow 2_{1,\text{ms}}^+$ | E2              | $740 \text{ e}^2\text{fm}^4$ [9]  | 38.1 mb                            | 558                                  |
|                     |                | $2_1^+ \rightarrow 2_{1,\text{ms}}^+$ | E2              | $20 \text{ e}^2\text{fm}^4$ [9]   |                                    |                                      |
|                     |                | $2_1^+ \rightarrow 2_{1,\text{ms}}^+$ | M1              | $0.51 \mu_N^2$ [9]                |                                    |                                      |

<sup>1</sup> calculated for ion kinetic energy at the center of the target

<sup>2</sup> energy loss taken into account, energy-dependent cross-section integrated over target-thickness

The execution of the experiment would be hindered if the beam would be significantly contaminated. In particular, a contamination of the  $^{136}\text{Te}$  beam with stable  $^{136}\text{Xe}$  might be a serious issue for a successful execution of the experiment. Therefore we request to use a selective laser-ionization scheme by means of RILIS and intend to measure in the well-known laser on/off-mode. In order to reduce the contamination predominantly due to  $^{136}\text{Xe}$ , the use of the Laser Ionization Source Trap (LIST) target, recently developed at ISOLDE [26], would be required. On the other hand, the extraction of molecular beams (Te oxide) from a  $\text{ThO}_2$  target that subsequently break-up in the REX-EBIS, REX-TRAP can also produce high purity  $^{136}\text{Te}$  beams and it is worth to be checked. In order to achieve a statistical accuracy of  $< 5\%$  in the Coulomb-excitation analysis, two days of beam on target are requested to collect the necessary amount of statistics

in the  $2_{1,\text{ms}}^+ \rightarrow 2_1^+$  transition. In addition, we ask for one day for testing the beam composition when extracting the molecular compounds and with the LIST target. The beam composition is determined by a) using the ionization chamber and b) implanting the beam into a thick target at the nominal secondary target position and observation of decay radiation with MINIBALL.

## 4 Summary

A projectile Coulomb excitation experiment on  $^{136}\text{Te}$  is proposed.

- Ions of  $^{136}\text{Te}$  will be produced in a standard  $\text{UC}_x/\text{graphene}$  target. The sufficiently pure production of the beam should either use extraction of molecular compounds or selective laser ionization. The beam intensity at the target position is expected to be  $10^5$  ions per second of  $^{136}\text{Te}$  with an energy of 510 MeV.
- A  $^{58}\text{Ni}$  target of a thickness of  $3 \text{ mg/cm}^2$  will be used, allowing us to perform a complementary lifetime analysis for the  $2_{1,\text{ms}}^+$  of  $^{136}\text{Te}$ .
- The standard DSSSD ("CD"-detector) will be used for the detection of scattered target ions.
- MINIBALL will be used for the detection of  $\gamma$  rays.

**Summary of requested shifts:** 3 shifts (one day) for beam production test and impurity analysis and 6 shifts (two days) for CE yield measurement in combined laser on/off mode

## References

- [1] F. Iachello, Phys. Rev. Lett. **53**, 1427 (1984).
- [2] N. Pietralla et al., Prog. Part. Nucl. Phys. **60**, 225 (2008).
- [3] K. Heyde and J. Sau, Phys. Rev. C **33**, 1050 (1986).
- [4] T. Ahn et al., Phys. Lett. B **679**, 19 (2009).
- [5] G. Rainovski et al., Phys. Rev. Lett. **96**, 122501 (2006).
- [6] J. D. Holt et al., Phys. Rev. C **76**, 034325 (2007).
- [7] V. Werner et al., Phys. Rev. C **78**, 031301 (2008).
- [8] M. Danchev et al., Phys. Rev. C **84**, 061306 (2011).
- [9] A.P. Severyukhin et al., Phys. Rev. C **90**, 011306 (2014).
- [10] D. C. Radford et al., et al., Phys. Rev. Lett. **88**, 222501 (2002).
- [11] L. Grodzins, Physics Letters **2**, 88 (1962).
- [12] R. F. Casten, Nucl. Phys. A **443**, 1 (1985).

- [13] J. Terasaki et al., Phys. Rev. C **66**, 054313 (2002).
- [14] N. Shimizu et al., Phys. Rev. C **70**, 054313 (2004).
- [15] A. Covello et al., Prog. Part. Nucl. Phys. **59**, 401 (2007).
- [16] N. Lo Iudice et al., Phys. Rev. C **77**, 044310 (2008).
- [17] D. Bianco et al., Phys. Rev. C **84**, 024310 (2011).
- [18] D. Bianco et al., Phys. Rev. C **85**, 034332 (2012).
- [19] D. Bianco et al., Phys. Rev. C **86**, 044325 (2012).
- [20] D. Bianco et al., Phys. Rev. C **88**, 024303 (2013).
- [21] M. Lettmann, Master's Thesis, TU Darmstadt (2013).
- [22] C. Stahl, Master's Thesis, TU Darmstadt (2012).
- [23] RILIS databse, URL: <http://riliselements.web.cern.ch/riliselements/>
- [24] ISOLDE yield information, URL: [https://oraweb.cern.ch/pls/isolde/query\\_tgt](https://oraweb.cern.ch/pls/isolde/query_tgt)
- [25] H. Geissel et al., URL: <http://web-docs.gsi.de/~weick/atima> (2011).
- [26] D. A. Fink et al., Nucl. Instr. Meth. B **417**, 417 (2013).



# Appendix

## DESCRIPTION OF THE PROPOSED EXPERIMENT

The experimental setup comprises: *MINIBALL + only CD, Ionization Chamber*

| Part of the                    | Availability                                 | Design and manufacturing  |
|--------------------------------|--|---|
| MINIBALL + only CD             | <input checked="" type="checkbox"/> Existing | <input checked="" type="checkbox"/> To be used without any modification   |
| Ionization chamber measurement | <input checked="" type="checkbox"/> Existing | <input checked="" type="checkbox"/> To be used without any modification<br><input type="checkbox"/> To be modified  |
|                                | <input type="checkbox"/> New                 | <input type="checkbox"/> Standard equipment supplied by a manufacturer<br><input type="checkbox"/> CERN/collaboration responsible for the design and/or manufacturing |
| Implantation & decay study     | <input checked="" type="checkbox"/> Existing | <input checked="" type="checkbox"/> To be used without any modification<br><input type="checkbox"/> To be modified  |
|                                | <input type="checkbox"/> New                 | <input type="checkbox"/> Standard equipment supplied by a manufacturer<br><input type="checkbox"/> CERN/collaboration responsible for the design and/or manufacturing |

HAZARDS GENERATED BY THE EXPERIMENT (if using fixed installation:) Hazards named in the document relevant for the fixed MINIBALL + only CD + Ionization Chamber installation.

Additional hazards:

| Hazards                               | MINIBALL + only CD        | Ionization chamber measurement | Implantation & decay study                   |
|---------------------------------------|---------------------------|--------------------------------|--|
| <b>Thermodynamic and fluidic</b>      |                           |                                |  |
| Pressure                              |                           |                                |  |
| Vacuum                                |                           |                                |  |
| Temperature                           |                           |                                |  |
| Heat transfer                         |                           |                                |  |
| Thermal properties of materials       |                           |                                |  |
| Cryogenic fluid                       |                           |                                |  |
| <b>Electrical and electromagnetic</b> |                           |                                |  |
| Electricity                           |                           |                                |  |
| Static electricity                    |                           |                                |  |
| Magnetic field                        |                           |                                |  |
| Batteries                             | <input type="checkbox"/>  |                                |  |
| Capacitors                            | <input type="checkbox"/>  |                                |  |
| <b>Ionizing radiation</b>             |                           |                                |  |
| Target material                       | $^{58}\text{Ni}$ , stable | No target                      | $^{197}\text{Au}$ or similarly heavy, stable |

|  |   |  |  |
|--|---|--|--|
| Beam particle type (e, p, ions, etc)                             | ions ( $^{136}\text{Te}$ )  | ions ( $^{136}\text{Te}$ )                 | ions ( $^{136}\text{Te}$ )                 |
| Beam intensity   | maximum available (below $10^7/\text{s}$ )                            | maximum available (below $10^7/\text{s}$ ) | maximum available (below $10^7/\text{s}$ ) |
| Beam energy  | 510 MeV   | 510 MeV                                    | 510 MeV                                    |
| Cooling liquids  |   |  |  |
| Gases  |   |  |  |
| Calibration sources:   | <input checked="" type="checkbox"/>                                   |  |  |
| • Open source  | <input checked="" type="checkbox"/> $^{241}\text{Am}$ / triple-Alpha  |  |  |
| • Sealed source  | <input checked="" type="checkbox"/> $^{60}\text{Co}, ^{152}\text{Eu}$ |  |  |
| • Isotope  |   |  |  |
| • Activity   |   |  |  |
| Use of activated material:                                       |   |  |  |
| • Description  | <input type="checkbox"/>  |  |  |
| • Dose rate on contact and in 10 cm distance                     |   |  |  |
| • Isotope  |   |  |  |
| • Activity   |   |  |  |
| <b>Non-ionizing radiation</b>                                    |   |  |  |
| Laser  |   |  |  |
| UV light   |   |  |  |
| Microwaves (300MHz-30 GHz)                                       |   |  |  |
| Radiofrequency (1-300 MHz)                                       |   |  |  |
| <b>Chemical</b>  |   |  |  |
| Toxic  |   |  |  |
| Harmful  |   |  |  |
| CMR (carcinogens, mutagens and substances toxic to reproduction) |   |  |  |
| Corrosive  |   |  |  |
| Irritant   |   |  |  |
| Flammable  |   |  |  |
| Oxidizing  |   |  |  |
| Explosiveness  |   |  |  |
| Asphyxiant   |   |  |  |
| Dangerous for the environment                                    |   |  |  |
| <b>Mechanical</b>  |   |  |  |
| Physical impact or mechanical energy (moving parts)              |   |  |  |

|   |  |  |  |
|---|--|--|--|
| Mechanical properties<br>(Sharp, rough, slippery) |  |  |  |
| Vibration   |  |  |  |
| Vehicles and Means of<br>Transport                |  |  |  |
| <b>Noise</b>                                      |  |  |  |
| Frequency   |  |  |  |
| Intensity   |  |  |  |
| <b>Physical</b>                                   |  |  |  |
| Confined spaces                                   |  |  |  |
| High workplaces                                   |  |  |  |
| Access to high work-<br>places                    |  |  |  |
| Obstructions in pas-<br>sageways                  |  |  |  |
| Manual handling                                   |  |  |  |
| Poor ergonomics                                   |  |  |  |

Hazard identification:

Average electrical power requirements (excluding fixed ISOLDE-installation mentioned above): 0 kW